DESIGN AND EXPERIMENT OF CLAMPING-PULL-OFF APPLE PICKING ROBOT
/
夹持-拉断式苹果采摘机器人设计与实验

Shike GUO, Min FU*, Xiaoman CUI, Zijan WANG, Chengmeng WANG
Northeast Forestry University, College of Mechanical and Electrical Engineering, Harbin / China;
Tel: +86 15663688203; E-mail: fumin1996@163.com
DOI: https://doi.org/10.35633/inmateh-71-22

Keywords: *apple; picking robot; clamping-pull-off type; kinematic analysis; trajectory planning.*

ABSTRACT

For the standardized apple orchards in China, which are mainly dwarfed and densely planted, firstly, according to the spatial distribution characteristics of fruits within the tree canopy, a clamping-pull-off apple picking robot was developed by analyzing the parameters of apple cultivation and picking methods, in order to replace the manual harvesting operation. Then, the Denavit-Hartenberg (DH) method was used to establish the kinematic Equations of the apple-picking robot, the forward and inverse kinematic calculations were carried out, and the Monte Carlo method was used to analyze the workspace of the robot. Through the robot picking task planning and the simulation of the trajectory of the robotic arm, the scheme of the robot's picking strategy was given, and MATLAB software was applied to simulate the motion trajectory as well as to verify the feasibility of the trajectory planning scheme and the picking strategy. Finally, an apple-picking test bed was set up, the corresponding picking control system program was designed, and 45 apples were selected for picking tests. The results showed that during the robot's picking process, the average time for picking each fruit was 7.59 seconds, the fruit recognition success rate was 86.67%, and the picking damage rate was 5.13%.

摘要

针对以矮化密植为主的中国标准化苹果园，首先根据树冠内果实空间分布特征，通过苹果栽培参数及采摘方法分析，开发出一种夹持-拉断式苹果采摘机器人，以代替人工采收作业。然后，通过 D-H 方法建立苹果采摘机器人运动学方程，并进行了正、逆运动学计算，并采用蒙特卡罗法分析了机器人作业空间。通过对机器人采摘任务规划及机械臂轨迹仿真，进一步给出了整机采摘轨迹的方案，并应用 MATLAB 软件对整机运动轨迹进行仿真，验证了轨迹规划方案和采摘策略的可行性。最后，搭建了苹果采摘试验台，设计出相应的采摘控制系统程序，并选取了 45 个苹果进行采摘测试。结果表明，该机器人采摘每个果实的平均时间为 7.59s，果实识别成功率为 86.67%，采摘损伤率为 5.13%。

INTRODUCTION

Rich in minerals and vitamins, apples are one of the fruits that are consumed regularly. China is a large apple-producing country in the world, the apple planting area in China covered 2.32 million hectares, accounting for 17.9% of the global total planting area, with an annual output of about 43 million tons *(Bu et al., 2020)*. In order to timely, efficiently, and carefully harvest apples, annual orchards require a large seasonal manual labor for harvesting, with labor costs accounting for about 66% of total costs. With the expansion of the apple planting industry, the conventional manual picking method struggles to meet the current market demand. In the face of an escalating labor shortage, the development of efficient and adaptable apple harvesting robots holds significant practical value *(Lan et al., 2022)*.

With the rapid development of information technology, agricultural mechanization is moving to the next new development stage, namely, agricultural precision *(Hou, 2020)*. Scholars have conducted a series of studies on fruit and vegetable picking robots for apples *(Jia et al., 2020; Zhang et al., 2019)*, strawberries *(Mejia et al., 2023; Xiong et al., 2019),* kiwis *(He et al., 2023; Wang et al., 2023)*, citrus *(Sun et al., 2023; Yin et al., 2023)*, and tomatoes *(Feng et al., 2018; Wang et al., 2023).* Improving the picking efficiency and non-destructive picking of picking robots are hot research topics *(Jia et al., 2020)*, and related scholars have proposed their own solutions. For example, Zhao et al., *(2020)*, designed a pneumatic hybrid-driven apple-picking robot, in which after localizing the fruit coordinates through the vision system, the end-effector used flexible gripping to capture the fruits and separate the fruit stalks with a cutter. The hybrid use of both electric and pneumatic drives significantly improved the picking efficiency of the robot, and the average time required for harvesting each fruit was 7.81 s, with a successful harvest rate of 81.25%.

Williams et al., *(2019)*, developed a kiwifruit four-arm picking robot with four arms mounted in parallel on a robotic platform. The picking sequence of the robotic arms was coordinated by the control system during the picking operations, greatly improving the efficiency of the robot's picking. The average time required for harvesting each fruit was 5.5 s, with a successful harvest rate of 51%.

The end-effector is one of the critical components of the picking robot *(Chen et al., 2023).* Considering the growth characteristics and picking requirements of various types of fruits, different structural forms of end-effectors should be designed to achieve efficient picking *(Fu et al., 2015)*. For example, considering the growth characteristics of strawberries cultivated on ridges, picking requires high flexibility. Therefore, *Zhang et al., (2023)*, designed a six-degree-of-freedom clamping strawberry-picking end-effector with a clamping mechanism equipped with blades to harvest the fruit by clamping off the fruit stalks. Considering the fragile epidermis of tomato fruits, *Chen et al., (2021)*, developed a pneumatic suction-clamp integrated three-jaw picking end-effector that utilized a pneumatic system to regulate the clamping force and picked the fruits through a four-step action of adsorption, pull-back, clamping, and twisting. Due to the compressive nature of the gas, the end-effector had a certain buffering and protective effect, reducing the damage rate of tomato fruits. Addressing citrus and other spherical fruits, *Xu et al., (2018)*, designed a suction navel orange picking end-effector, using a suction cup to extract the fruit and then separating the fruit from the stalk with a cutter. The above research provides useful insights for the development of apple and other fruit and vegetable picking technology, but most of the current apple-picking end-effectors have certain limitations and are not adapted to picking fruits of different shapes, sizes, and various postures in any environment, i.e., the versatility is weak.

Given the above analysis, this paper focused on the typical standardized apple orchard working conditions in China and designed an apple-picking robot suitable for picking fruits of various shapes and sizes. Firstly, MATLAB software was performed to conduct forward and reverse kinematics analysis of the apple-picking robot, and the robot's workspace range was determined. Then, by planning the picking task and simulating the trajectory of the robotic arm, the picking strategy was formulated. Finally, an apple-picking test bed was established to verify the working efficiency of the apple-picking robot.

MATERIALS AND METHODS

Background

China’s standardized apple orchards feature dwarfed and densely planted trees with a high spindle shape, providing advantages such as a compact tree shape, open space in tree rows, good ventilation and light penetration, and ease of mechanized operations. As shown in Figure 1, the row spacing of fruit trees is about 3.0~4.0 m, with fruit tree heights generally ranging from 2.5~3.0 m, crown widths of 1.0~1.5 m, thicknesses of about 0.5~1.0 m, and a range of depths of fruit distributions of 0~0.4 m. Statistically, about 90% or more of the fruits are distributed at a height of 0.6-2.6 m *(Feng et al., 2023)*. According to the growth condition of dwarfed apple trees, it is determined that the target horizontal working space of the picking robotic gripper is 0~1.5 m, with a vertical working space of 0.5~2.8 m.

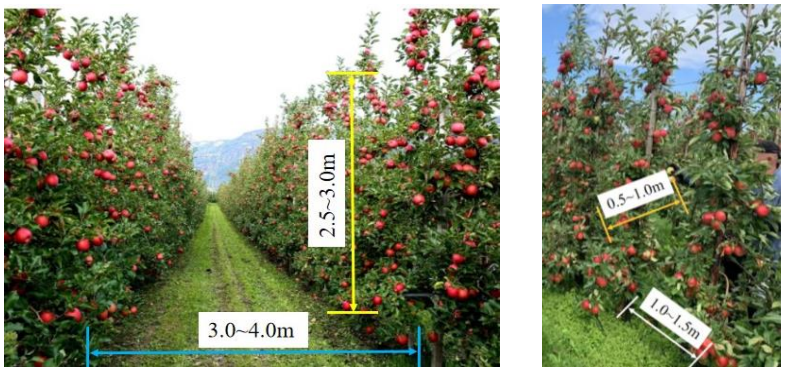

Fig. 1 - Dwarf and dense planting standard orchard

Fruit harvesting methods

During the process of picking apples, the end-effector first carries out the grasping action, targeting either the fruit or the fruit stalk. The main methods of capture include the clamping type and the suction type. After completing the gripping action, the fruits need to be separated from the fruit trees, with separation methods typically involving cutting, pulling, and twisting.

Following fruit picking, the primary methods of fruit collection include putting back, throwing down, and pipe collection. The specific analysis of the implementation of each stage is shown in Table 1.

Table 1

End-effector harvesting action methods

	Action	Principle	Characteristic
Capturing fruit method	Grab	Simulating the human hand to grab the fruits	Suitable for capturing fruits of all sizes
	Suck	Sucking the fruits, the end-effector by negative pressure	Suitable for capturing small shaped fruits
Separating fruit stalks method	Cut	Cutting the fruit stalks by means of cutters	Low damage to fruits and plants, but complicated control system
	Pull	Using external force to pull and break the fruit stalks	The operation is simple, but requires control of the force of pulling off the fruit stalks
	Twist	Using external force to twist off the fruit stalks	Rapidly twist off fruit stalks, but easily damages fruit skins
Collecting fruits method	Put back	Using a robotic arm to place fruits into a collection device	Reducing fruit damage but is time consuming
	Throw down	Releasing the fruit directly after picking it from the tree	Easy and convenient to operate, but easy to damage the fruit
	Pipeline	The fruit falls into the collection device through a pipeline	Fruits collection is efficient, but requires the design of piping to match the machine

After comparative analysis, grabbing is used to capture apples, pulling off to separate the stalks, and placing to collect the fruits. The geometric model of the apple-picking method is shown in Figure 2.

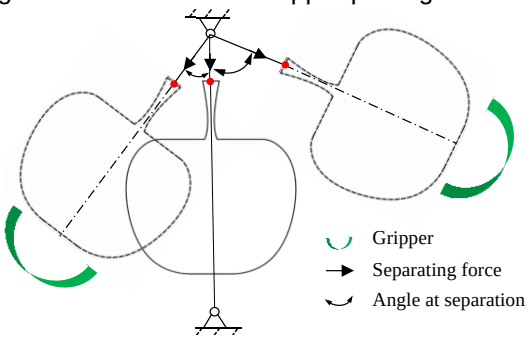

Fig. 2 - Geometric model of apple picking method

In manual harvesting operations, apples are picked in such a way that the stalks are pulled directly off the branches. The resulting tensile force pulls off the fruit stalks by tending to separate the fruit from the branch relative to each other. Inspired by the manual harvesting methods described above, the law of the separation of apple fruits from fruit stalks was investigated in a preliminary stage. From the study in reference *Chen et al., (2022)*, it can be observed that when the fruit stalk was separated from the branch at an arbitrary angle without damaging the fruit, the tensile force at separation increased with the increase of the apple diameter, within a range of 8.88 N to 39.6 N. Additionally, the maximum pressure an apple can withstand was found to be 15.35 N after an apple resistance test. Therefore, in this paper, to reduce the damage rate of the fruits during picking and to ensure the quality of the fruits, the clamping force when picking the fruits is set to 15.35 N, and the pulling force when separating the fruit stalks is set to 40 N.

Structure and working principle of the whole machine

The overall structure of the apple-picking robot is shown in Figure 3, mainly consisting of a robotic gripper, RGB-D camera, robotic arm, fruit collection box, support frame, navigation camera, and crawler chassis. While working, the robot first performs system initialization. Then, the robot localizes the fruit tree through the navigation system and stops when it reaches the position of the fruit tree. The RGB-D camera starts scanning the surroundings and, after recognizing the presence of apples nearby, the robotic arm carries the robotic gripper to hold the apples with the preset gripping force and uses a pulling and tugging method to pick the apples from the fruit tree. Finally, the robotic arm takes the robotic gripper and places the picked apples into the fruit collection box, completing the single-picking process.

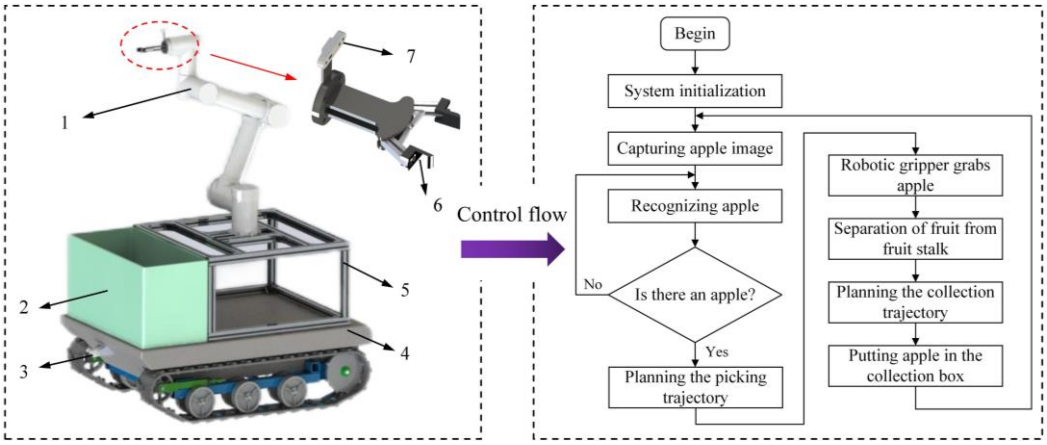

Fig. 3 - Structure and control flow of the apple picking robot

1. six-degree-of-freedom robotic arm 2. fruit collection box 3. navigation camera 4. crawler chassis 5. support frame 6. robotic gripper; 7. RGB -D camera

KINEMATIC ANALYSIS

Robot kinematics is primarily concerned with analyzing the relationship between the position of the end-effector and the joint variables of the robotic arm *(Wang et al., 2020)*. This chapter lays the foundation for the trajectory planning and picking strategy for robot by calculating the forward and inverse solutions of the robot kinematics and analyzing the workspace.

Forward kinematic analysis

The kinematic equations of the apple-picking robot were established using the Denavit-Hartenberg (DH) parameter method, and the connecting rod coordinates are shown in Figure 4. The D-H parameters for each joint were determined based on the connecting rod parameters and the relationships within the established coordinate system, as shown in Table 2.

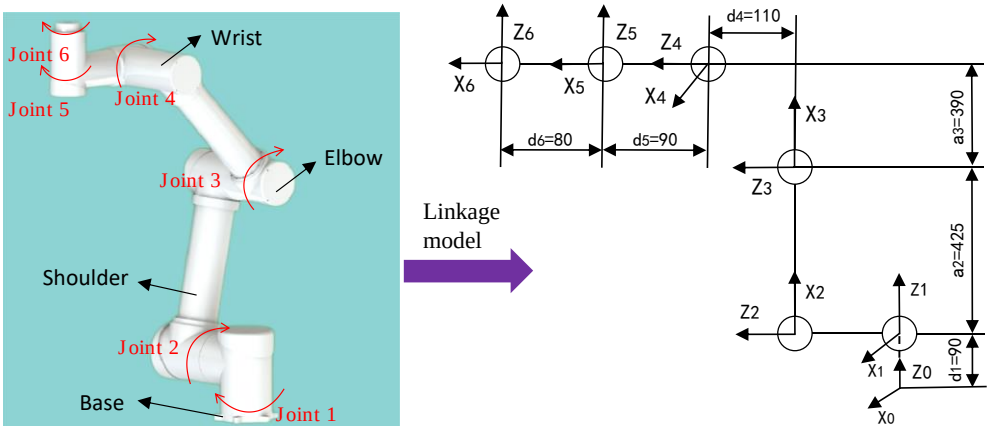

Fig. 4 - The connecting rod coordinate system

Table 2

Parameters of the apple-picking robot

i	α_i / (°)	a_i / mm	d_i / mm	θ_i/(°)	Variable Range
1	90	0	90	θ_1	-360~360
2	0	425	0	θ_2	-90~90
3	0	390	0	θ_3	-180~180
4	90	0	110	θ_4	-30~30
5	-90	0	90	θ_5	-90~90
6	0	0	80	θ_6	-90~90

where: i is the number of joints, α_i, is the rotation angle of the connecting rod, a_i is the length of the connecting rod, d_i is the offset distance of the connecting rod and θ_i is the joint angle. θ_1, θ_2, θ_3, θ_4, θ_5, and θ_6 are joint angle variables.

The transformation matrix between neighboring connecting rod coordinate systems is:

$$ {}^{i-1}_{i}T = \begin{bmatrix} cos\theta_i & -sin\theta_i cos\alpha_i & sin\theta_i sin\alpha_i & a_i cos\theta_i \\ sin\theta_i & cos\theta_i cos\alpha_i & -cos\theta_i sin\alpha_i & a_i sin\theta_i \\ 0 & sin\alpha_i & cos\alpha_i & d_i \\ 0 & 0 & 0 & 1 \end{bmatrix} \quad (1) $$

where:

${}^{i-1}_{i}T$ represents the Homogeneous transformation matrix of the connecting rod relative to the connecting rod $i-1$.

According to the principle of forward kinematics, each connecting rod transformation matrix can be obtained by substituting each connecting rod parameter from Table 2 into Equation (1).

Where the apple- picking robot equation of motion ${}^{0}_{6}T$ is expressed as the position of the end-effector with respect to the base coordinate system:

$$ {}^{0}_{6}T = {}^{0}_{1}T\,{}^{1}_{2}T\,{}^{2}_{3}T\,{}^{3}_{4}T\,{}^{4}_{5}T\,{}^{5}_{6}T = \begin{bmatrix} n_x & o_x & a_x & p_x \\ n_y & o_y & a_y & p_y \\ n_z & o_z & a_z & p_z \\ 0 & 0 & 0 & 1 \end{bmatrix} \quad (2) $$

Among them:

$$ \begin{cases} n_x = c_6\left(s_1 s_5 + c_5 c_1 c_{234}\right) - s_6 c_1 s_{234} \\ n_y = c_6\left(c_5 s_1 c_{234} - c_1 s_5\right) - s_6 s_5 s_{234} \\ n_z = c_5 c_6 s_{234} + s_6 c_{234} \\ o_x = -s_6\left(c_5 c_1 c_{234} + s_1 s_5\right) - c_6 c_1 s_{234} \\ o_y = -s_6\left(c_5 s_1 c_{234} - c_1 s_5\right) - c_6 s_1 s_{234} \\ o_z = c_6 c_{234} - c_5 s_6 s_{234} \\ a_x = -s_5 c_1 c_{234} + c_5 s_1 \\ a_y = -s_5 s_1 c_{234} - c_1 c_5 \\ a_z = -s_5 s_{234} \\ p_x = 90 c_1 s_{234} + 110 s_1 + 80\left(c_5 s_1 - s_5 c_1 c_{234}\right) + 425 c_1 c_2 + 390 c_1 c_{23} \\ p_y = 90 s_1 s_{234} - 110 c_1 - 80\left(s_5 s_1 c_{234} + c_1 c_5\right) + 425 c_2 s_1 + 390 s_1 c_{23} \\ p_z = 90 - 90 c_{234} + 425 s_2 + 390 s_{23} - 80 s_5 s_{234} \end{cases} \quad (3) $$

where:

c_i is an abbreviation of $cos\theta_i$, s_i is an abbreviation of $sin\theta_i$, $cos(\theta_i + \theta_j) = c_{ij}$, $sin(\theta_i + \theta_j) = s_{ij}$.

Inverse kinematic analysis

The kinematic inverse solution is that the angle of each joint is calculated by knowing the position and attitude of the robot's end-effector to achieve precise positioning and control of the robot. In this section, the matrix inverse multiplication analytic method was used to solve the kinematic inverse solution of the apple picking robot.

The values of the joint variables are solved in turn according to the analytic method as:

$$ \theta_1 = A\tan 2(80a_y - p_y, 80a_x - p_x) - A\tan 2\left(110, \pm\sqrt{(80a_y - p_y)^2 + (80a_x - p_x)^2 - 110^2}\right) \quad (4) $$

$$ \theta_2 = A\tan 2\left(\frac{(a_3c_3 + a_2)n - a_3 s_3 m}{a_2^{\,2} + a_3^{\,2} + 2a_2 a_3 c_3}, \frac{m + a_3 s_3 s_2}{a_3 c_3 + a_2}\right) \quad (5) $$

$$ \theta_3 = \pm\arccos\left(\frac{m_2 + n_2 - a_2^{\,2} - a_3^{\,2}}{2a_2 a_3}\right) \quad (6) $$

$$ \theta_4 = A\tan 2\left(-s_6\left(n_x c_1 + n_y s_1\right) - c_6\left(o_x c_1 + o_y s_1\right), o_z c_6 + n_z s_6\right) - \theta_2 - \theta_3 \quad (7) $$

$$\theta_5 = \pm \arccos\left(a_x s_1 - a_y c_1\right) \tag{8}$$

$$\theta_6 = A\tan 2\left(\frac{n_x s_1 - n_y o_x}{s_5}, \frac{o_x s_1 - o_y c_1}{s_5}\right) \tag{9}$$

where:

$$\begin{cases} m = 90\left(s_6\left(n_x c_1 + n_y s_1\right) + c_6\left(o_x c_1 + o_y s_1\right)\right) - 90\left(a_x c_1 + a_y s_1\right) + p_x c_1 + p_y s_1 \\ n = p_z - 90 - 80a_z + 90\left(o_z c_6 + n_z s_6\right) \end{cases}$$

Workspace analysis

The workspace is the collection of spatial points that can be reached by the end-effector during the picking process of the robot, and its shape and size are the key factors that determine the robot's work performance. Based on the Robotics Toolbox in MATLAB software, the Monte Carlo method was used to solve the approximate solution in motion space *(Xu et al., 2018).*

Through the forward kinematics Equation (2), the position vector of the end-effector relative to the base was solved, and then multiple end position coordinate points were randomly generated by the Rand function to obtain the workspace as shown in Figure 5.

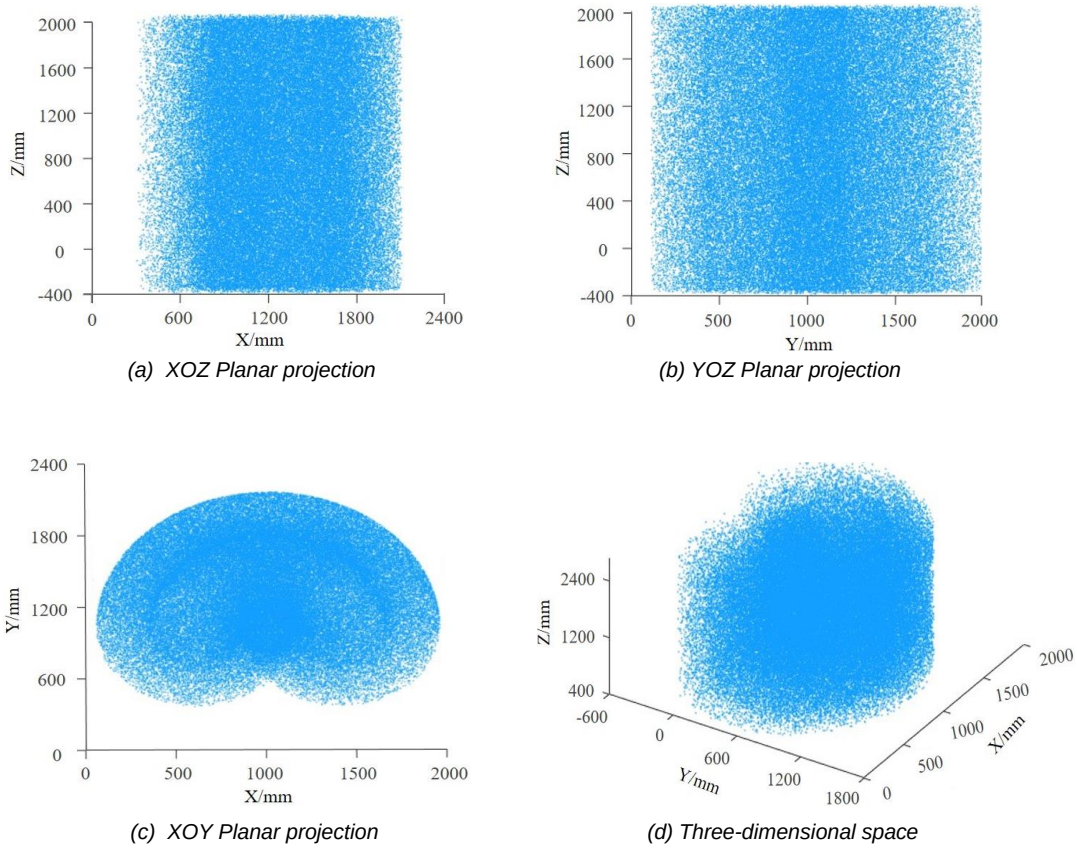

(a) XOZ Planar projection *(b) YOZ Planar projection*

(c) XOY Planar projection *(d) Three-dimensional space*

Fig. 5 -Workspace of the apple-picking robot

From Figure 5, the workspace of the apple-picking robot is a heart-like columnar space, X-direction travel is about 1.4 m; Y-direction travel is about 1.8 m; and Z-direction travel is about 2.0 m. The simulation results provide the foundation for the trajectory planning of the robotic arm and the design of the picking strategy in the subsequent section.

The dexterous workspace of the apple-picking robot is shown in Figure 6. The space avoids collisions between the robotic arm and the internal branches of the apple tree, as well as interference between the arm and the mechanics of the robot. During the actual picking task, the position of the picked apples should be within the dexterity workspace.

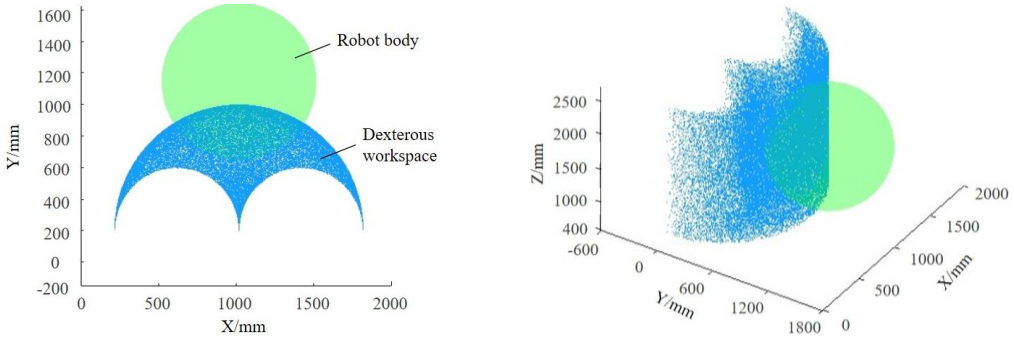

(a) XOY Planar projection *(b) Three-dimensional space*

Fig. 6 -Space for dexterous work

PICKING TRAJECTORY PLANNING

Picking task planning

When the robot has finished picking apple $i-1$ and will pick apple i, the picking motion can be divided into three phases:

(1) Leaving the apple $i-1$ place, avoiding branches and leaves.

(2) Moving within a safe area where there will be no collision with the branching vine, approaching the target apple i.

(3) Arriving at the target apple i, the robotic gripper performs the picking.

During the transfer of the picking target, it was necessary to ensure that the branches of the fruit tree don't interfere with the robot. During trajectory planning, a safety point H was added to split the motion of the second stage into two parts to ensure that the positional transitions of the robotic arm could take place in a safe area. As a result, each picking task involved the planning of four trajectory segments and five points, as shown in Figure 7.

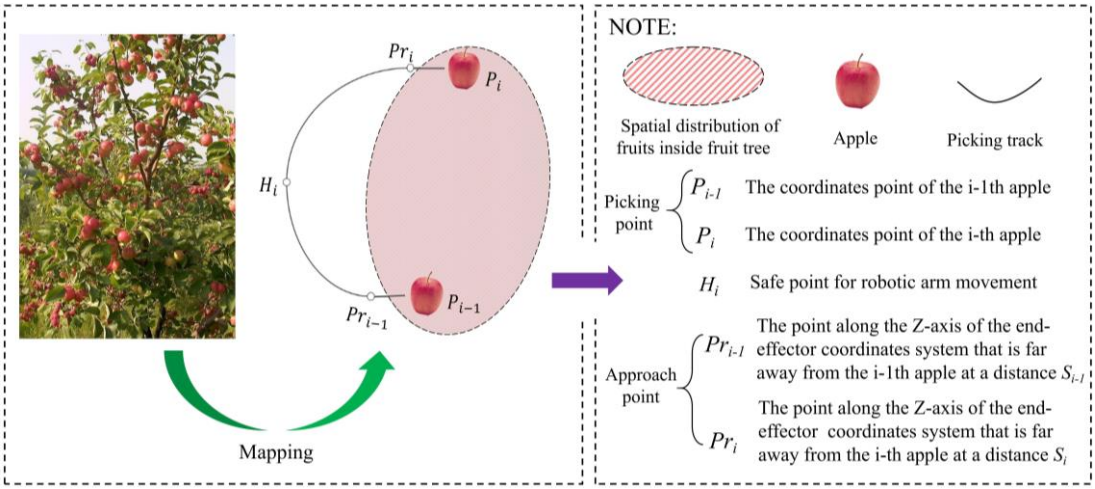

Fig. 7 - Trajectory planning node between two picks

When $i \neq 0$, the robot has just finished picking apple $i-1$ and will pick apple i. The path for trajectory planning is:

$$P_{i-1} \rightarrow Pr_{i-1} \rightarrow H_i \rightarrow Pr_i \rightarrow P_i$$

When $i = 0$, the robot has just started to work, the robot arm is in the zero position, and the coordinates' position of the end-effector is the point H at this time. The path for trajectory planning is:

$$H_0 \rightarrow Pr_0 \rightarrow P_0$$

Trajectory planning of the robotic arm

The purpose of robotic arm trajectory planning is to ensure that the position, velocity, and acceleration function curves of each joint variable are continuous and smooth during the completion of operational tasks *(Yang et al., 2020)*.

Common robot trajectory planning methods today include trapezoidal planning, S-planning, and polynomial planning. Among these, polynomial planning is the most commonly used, with a mature planning method that ensures the continuity of displacement, velocity, and acceleration in the planning process, allowing for smooth robot movement. Therefore, in this paper, the fifth-degree polynomial interpolation method was used, and the MATLAB Robotics toolbox was invoked to simulate joint space trajectory planning for any two points in the robot end-effector space.

A time-varying function is utilized to represent each joint variable during joint space trajectory planning, by which the process of trajectory change of the robot over a certain period of time is illustrated. The start point coordinate q_0 and end point coordinate q_1 of the robot are given. Utilizing the jtraj function, the call format is:

$$\begin{bmatrix} q & qd & qdd \end{bmatrix} = jtraj(q_0, q_1, t) \tag{10}$$

where: q stands for displacement; qd stands for velocity; qdd stands for acceleration; t stands for simulation time.

The $function\,jtraj$ is a fifth-degree polynomial interpolation, with default initial and final velocities set to zero. The simulation time was 2 s, and the jtraj function was called to observe the motion change process of each joint. The plot function was then used to generate the displacement, angular velocity, and angular acceleration curves of the robot, as shown in Figure 8.

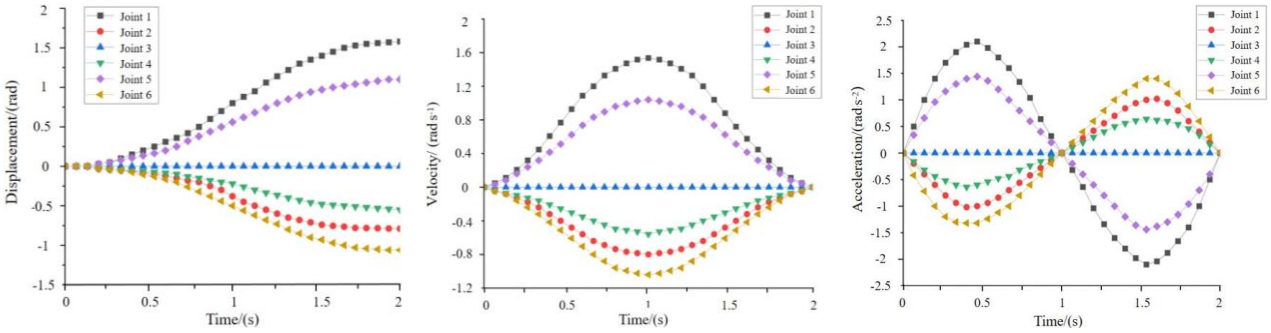

(a) displacement curve *(b) velocity curve* *(c) acceleration curve*

Fig. 8 - Dynamics of the joints over time

Figure 8(a) reflects the movement process of each joint over time. Figure 8(b) reflects the velocity variation of each joint over time, and they satisfy the requirement that the starting and ending velocities of the fifth-degree polynomial interpolation are all zero. The change in acceleration for each joint is depicted in Figure 8(c) and the curved motion is smooth without abrupt changes. Velocity and acceleration curves are smooth and excessive, without inflection points, interruptions, jumps, and other phenomena, indicating that the robot ran smoothly.

Dynamic simulation of picking trajectory

Based on kinematic forward and inverse solutions, as well as workspace analysis of the apple-picking robot, MATLAB simulation software was utilized to simulate the entire motion trajectory of the apple-picking robot. Two apples, positioned at different heights on an apple tree, were chosen as examples (the brown area represents the apple tree, and the red area represents the apples) to simulate the growing environment of apples in an orchard. The simulation results are shown in Figure 9.

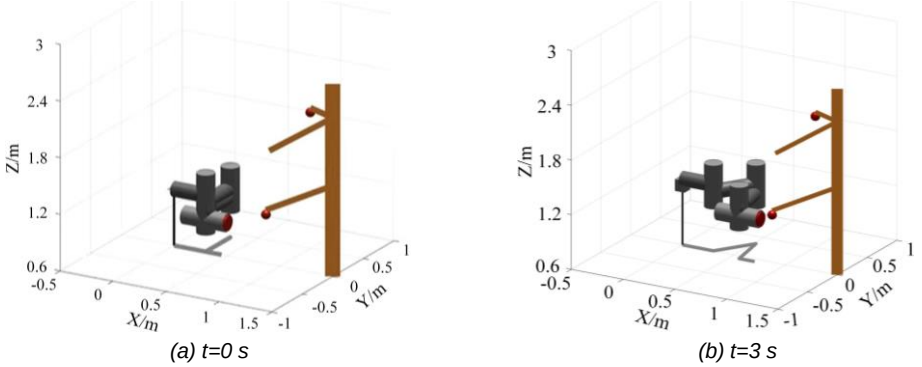

(a) t=0 s *(b) t=3 s*

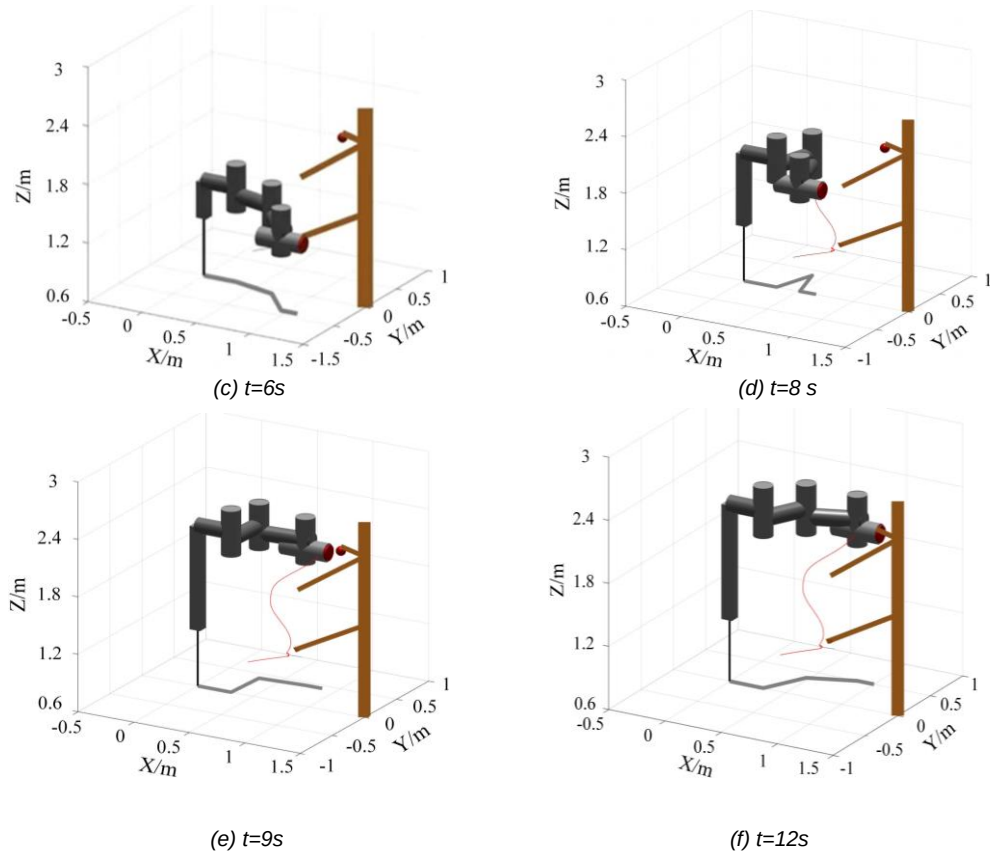

Fig. 9 - Dynamic simulation of the picking trajectory

The entire process took 12 s, starting from the recognition of the first apple to the completion of the second apple picking. At t = 0 s, the robot was in the initial state. From 1 to 3 s, the robot recognized the first apple and proceeded to pick it. Between 3 and 6 s, the robotic gripper successfully completed the picking of the first apple by clamping the fruit and pulling off the stalk. From 7 to 12 s, after navigating around branch obstacles, the robot recognized the second apple and completed the picking process. The simulation results showed that the robot took 6 s from the beginning of recognizing the first fruit to completing the picking, and then took 3 s to recognize the second fruit. During the fruit picking process, the entire picking trajectory of the machine met the requirements of the apple picking workspace, which verified the feasibility of the trajectory planning scheme and the picking strategy.

RESULTS

Control systems design

A picking test bed was set up in the laboratory environment for the apple picking test, and its hardware platform mainly includes robotic gripper, a robotic gripper, an RGB-D camera, an upper computer, and a control cabinet, as shown in Figure 10(a).

The upper computer is mainly responsible for running the main program of the control system, including acquiring and processing platform data and controlling platform equipment. The RGB-D camera is mainly responsible for providing real-time image data of scene objects and distance information included in the depth image data. The robotic gripper is mainly responsible for driving the robotic gripper to the designated position and cooperating with it to complete the corresponding action.

In addition, C+ + was used as the programming language in this paper, and MDK software was used for programming and debugging to design the picking control system program.

According to the working principle and operation flow of the robot, the visual recognition and localization module flow (see Figure 10(b)), the robotic gripper motion control module flow (see Figure 10(c)), and the robotic gripper motion control module flow (see Figure 10(d)) have been designed for controlling the hardware devices, such as the RGB-D camera, the robotic arm, and the robotic gripper.

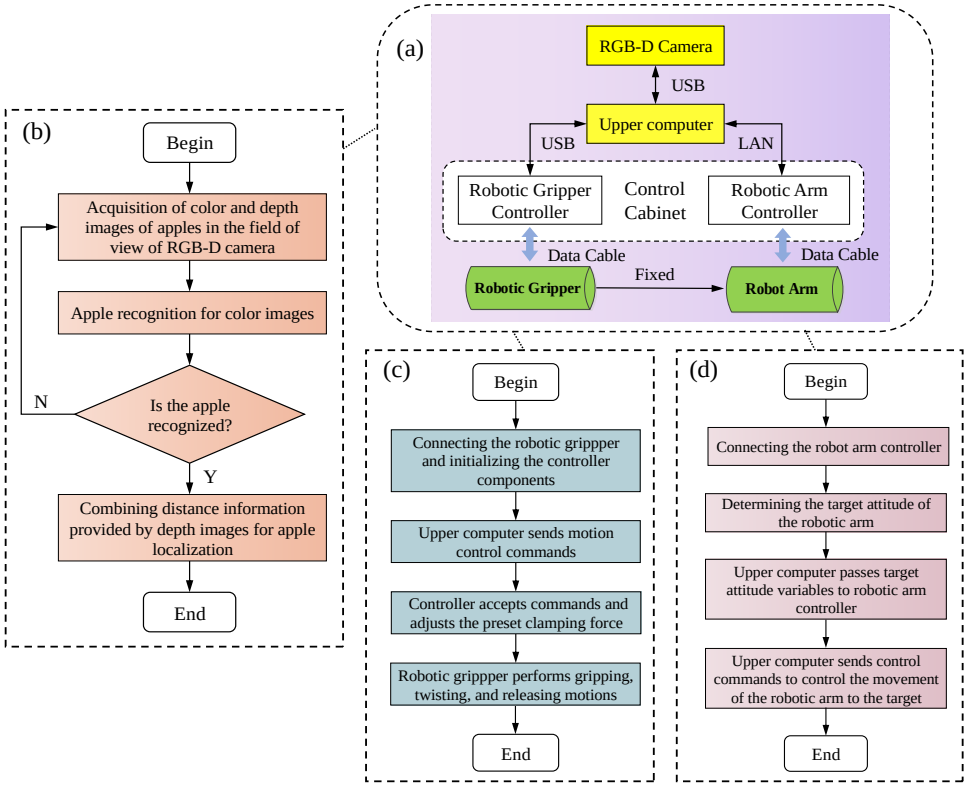

Fig. 10 - Hardware platform of the picking robot and the control flow of each module

(a). hardware platform; (b). control module of visual recognition and localization; (c). control module of the robotic gripper; (d). control module of the robotic arm

Results and analysis

The picking test was carried out on September 10, 2023, in a laboratory setting, as shown in Figure 11. Forty-five apples with an average fruit diameter of 72 mm were selected at the beginning of the test and placed at different heights of the fruit tree to verify the harvesting performance of the robot. During the work, the robotic arm was set to move at a speed of 1.5 m/s and separate the fruit stalks with a pulling force of 40 N, and the robotic gripper was set to hold the apples with a gripping force of 15.35 N. During the picking process, the robot first scanned the surroundings with an RGB-D camera, and after recognizing the apples, the robotic gripper gripped the apples with a preset gripping force. Then, the robotic arm carried the robotic gripper to pick the apples from the fruit tree in a pulling and tugging manner and carried the robotic gripper to put the picked apples into the collection box.

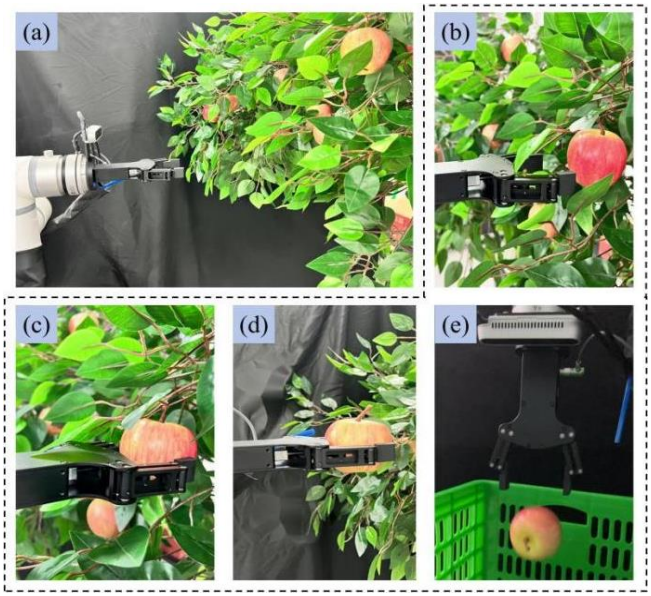

Fig. 11 - Apple picking process

(a). test Scenarios (b). recognizing apples (c). clamping apples at a preset clamping force (d). pulling off the stalks (e). collecting apples

Three picking tests were conducted from different angles of the fruit tree, and the results showed that the robot successfully recognized 39 fruits, with a recognition success rate of 86.67%. The robot collected 37 fruits without damage, resulting in a damage rate of 5.13%. The average time for picking each fruit was 7.59 seconds, of which the average time spent in the process of recognizing the fruits and moving to the picking stage was 3.26 seconds, while the average time spent in the process of picking and collecting the fruits was 4.33 seconds.

The reason for the failure of fruit picking in the test could be that some fruits were closer to the inner contour of the fruit tree and were obscured by branches and leaves, resulting in the RGB-D camera failing to recognize these fruits. In addition, the cause of fruit damage might be that when picking fruits that were too small in diameter, the preset gripping force exceeded the range of pressure that the fruit could withstand, resulting in the fruit being damaged by the robotic gripper.

CONCLUSIONS

(1) Taking Chinese dwarf anvil densely planted high spindle fruit trees as an object, a clamping-pull-off apple-picking robot was designed by analyzing apple cultivation parameters and picking methods. Firstly, the kinematic equations of an apple-picking robot were established by the D-H method, and forward and inverse kinematic calculations were performed. The robot reachable workspace and dexterous workspace ranges were solved using Robotics Toolbox in MATLAB software and the Monte Carlo method. Secondly, through the robot picking task planning and the simulation of the trajectory of the robotic arm, furthermore, the scheme of the robot's picking strategy was given. Finally, MATLAB was applied to simulate the motion trajectory of the apple-picking robot, validating the feasibility of the trajectory planning scheme and the picking strategy.

(2) An apple picking test bed was set up in the laboratory environment, and a corresponding picking control system program was designed based on the robot's working principle and workflow. Forty-five apples were selected and positioned at various heights on the fruit tree for picking tests. The results indicated that, during the robot's picking process, the average time for picking each fruit was 7.59 seconds, with a fruit recognition success rate of 86.67% and a picking damage rate of 5.13%.

ACKNOWLEDGEMENT

This paper was funded by the National Natural Science Foundation of China (Grant No.51975114).

REFERENCES

[1] Bu, L. X., Chen, C. K., Hu, G. R., Sugirbay, A., & Chen, J. (2020). Technological development of robotic apple harvesters: A review. *INMATEH-Agricultural Engineering*, 61(2), 151-164.

[2] Chen, K., Li, T., Yan, T., Xie, F., Feng, Q., Zhu, Q., & Zhao, C. (2022). A soft gripper design for apple harvesting with force feedback and fruit slip detection. *Agriculture*, 12(11), 1802.

[3] Chen, Q., Yin, C. K., Guo, Z. L., Wang, J. P., Zhou, H. P., & Jiang, X. S. (2023). Research status and development trend of apple picking robot key technology (苹果采摘机器人关键技术研究现状与发展趋势). *Transactions of the Chinese Society of Agricultural Engineering*, 39(04), 1-15.

[4] Chen, Z. W., Yang, M. J., Li, Y. W., & Yang, L. (2021). Design and test of tomato picking end-effector based on pneumatic non-destructive clamping control (基于气动无损夹持控制的番茄采摘末端执行器设计与试验). *Transactions of the Chinese Society of Agricultural Engineering*, 37(02), 27-35.

[5] Feng, C. C., Zhao, C. J., Li, T., Chen, L. P., Guo, X., Xie, F., et al. (2023). Design and testing of a four-arm apple picking robot system (苹果四臂采摘机器人系统设计与试验). *Transactions of the Chinese Society of Agricultural Engineering*, 39(13), 25-33.

[6] Fu, L., Zhang, F., Gejima, Y., Li, Z., Bin, W., & Cui, Y. (2015). Development and experiment of end-effector for kiwifruit harvesting robot (猕猴桃采摘机器人末端执行器设计与试验). *Transactions of the Chinese Society of Agricultural Machinery*, 46(3).

[7] Feng, Q., Zou, W., Fan, P., Zhang, C., & Wang, X. (2018). Design and test of robotic harvesting system for cherry tomato. *International Journal of Agricultural and Biological Engineering*, 11(1), 96-100.

[8] He, Z., Li, Z. X., Ding, X. T., Li, K., Shi, Y. G., & Cui, Y. J. (2023). Design and experiment of end effect for kiwifruit harvesting based on optimal picking parameters. *INMATEH-Agricultural Engineering*, 69(1).

[9] Hou, Z. (2020). Analysis of visual navigation extraction algorithm of farm robot based on dark primary colour. *INMATEH-Agricultural Engineering*, 62(3).

[10] Jia, W., Tian, Y., Luo, R., Zhang, Z., Lian, J., & Zheng, Y. (2020). Detection and segmentation of overlapped fruits based on optimized mask R-CNN application in apple harvesting robot. *Computers and Electronics in Agriculture*, 172, 105380.

[11] Jia, W., Zhang, Y., Lian, J., Zheng, Y., Zhao, D., & Li, C. (2020). Apple harvesting robot under information technology: A review. *International Journal of Advanced Robotic Systems*, 17(3), 1729881420925310.

[12] Lan, Y., Yan, Y., Wang, B., Song, C., & Wang, G. (2022). Current status and future development of the key technologies for intelligent pesticide spraying robots (智能施药机器人关键技术研究现状及发展趋势). *Transactions of the Chinese Society of Agricultural Engineering*, 38, 30-40.

[13] Mejia, G., de Oca, A. M., & Flores, G. (2023). Strawberry localization in a ridge planting with an autonomous rover. *Engineering Applications of Artificial Intelligence*, 119, 105810.

[14] Sun, Q., Zhong, M., Chai, X., Zeng, Z., Yin, H., Zhou, G., & Sun, T. (2023). Citrus pose estimation from an RGB image for automated harvesting. *Computers and Electronics in Agriculture*, 211, 108022.

[15] Wang, K., Zhang, W., Luo, Z. & Zhang, Y. (2020). Design and experiment of hitting pine cone picking robot (击打式松果采摘机器人设计与试验). *Transactions of the Chinese Society for Agricultural Machinery*, 51(8), 26-33.

[16] Wang, T., Du, W., Zeng, L., Su, L., Zhao, Y., Gu, F., Li, L., & Chi, Q. (2023). Design and Testing of an End-Effector for Tomato Picking. *Agronomy*, 13(3), 947.

[17] Wang, Y., He, Z., Cao, D., Ma, L., Li, K., Jia, L., & Cui, Y. (2023). Coverage path planning for kiwifruit picking robots based on deep reinforcement learning. *Computers and Electronics in Agriculture*, 205, 107593.

[18] Williams, H. A., Jones, M. H., Nejati, M., Seabright, M. J., Bell, J., Penhall, N. D., et al. (2019). Robotic kiwifruit harvesting using machine vision, convolutional neural networks, and robotic arms. *Biosystems Engineering*, 181, 140-156.

[19] Xiong, Y., Peng, C., Grimstad, L., From, P. J., & Isler, V. (2019). Development and field evaluation of a strawberry harvesting robot with a cable-driven gripper. *Computers and electronics in agriculture*, 157, 392-402. https://doi.org/10.1016/j.compag.2019.01.009

[20] Xu, L., Liu, X., Zhang, K., Xing, J., Yuan, Q., Chen, J., et al. (2018). Design and test of end-effector for navel orange picking robot (脐橙采摘机器人末端执行器设计与试验). *Transactions of the Chinese Society of Agricultural Engineering*, 34(12), 53-61.

[21] Xu, Z. B., Zhao, Z. Y., He, S., He, J. P., & Wu, Q. W. (2018). Improvement of Monte Carlo method for robot workspace solution and volume calculation (机器人工作空间求解的蒙特卡洛法改进和体积求取). *Optics and Precision Engineering*, 26(11), 2703-2713.

[22] Yang, C. G., Cheng, L., & Li, J. (2020). Robot control - kinematics, controller design, human-robot interaction and application examples (机器人控制–运动学、控制器设计、人机交互与应用实例). *Tsinghua University Press*: Beijing, China, pp.40-53.

[23] Yin, H., Sun, Q., Ren, X., Guo, J., Yang, Y., Wei, Y., Huang, B., Chai, X., & Zhong, M. (2023). Development, integration, and field evaluation of an autonomous citrus-harvesting robot. *Journal of Field Robotics*.

[24] Zhao, D., Wu, R., Liu, X., Zhang, X., & Ji, W. (2020). Design and Experiment of Apple Harvesting Robot Based on Gas-electric Hybrid Drive (气电混合驱动全天候苹果收获机器人设计与试验). *Transactions of the Chinese Society of Agricultural Machinery*, 51(2).

[25] Zhang, Y., Tian, Y., Zheng, C., Zhao, D., Gao, P., & Duan, K. (2019). Segmentation of apple point clouds based on ROI in RGB images. *INMATEH-Agricultural Engineering*, 58(3).

[26] Zhang, Y., Zhang, K., Yang, L., Zhang, D., Cui, T., Yu, Y., & Liu, H. (2023). Design and simulation experiment of ridge planting strawberry picking manipulator. *Computers and Electronics in Agriculture*, 208, 107690.